#### **Research Article**

Zuhur Algahtani, Ibrahim Abbas\*, Alaa A. El-Bary, Areej Almuneef

# Thermoelastic interactions in functionally graded materials without energy dissipation

 $c_e$ 

https://doi.org/10.1515/cls-2024-0023 received August 20, 2024; accepted November 17, 2024

Abstract: This study addresses the problem of thermoelastic interaction in functionally graded isotropic unbounded media owing to a timed pulse within the framework of generalized thermoelastic theory without energy dissipation (TEWOED). Functionally graded material (FGM, or material with spatially variable material characteristics) has its governing equations for the generalized thermoelastic model without energy dissipation (GNII) developed. These formulations are expressed in terms of Laplace transforms. The analytical solutions in the transform's domain are obtained through the eigenvalues technique. The Laplace transforms are inversed using numerical methods. Finally, the acquired data are visually illustrated to illustrate how inhomogeneity, laser intensity, and laser pulse length affect displacement, temperature, and stress.

**Keywords:** functionally graded material, eigenvalues approach, Laplace transform, laser pulse length, without energy dissipation

## **Nomenclature**

 $\delta$  Absorption depth of heating energy

 $u_i$  Displacement components

Q External heat source

*T<sub>o</sub>* Initial temperature of medium

 $\delta_{ij}$  Kronecker symbol  $\lambda, \mu$  Lame's constants

\* Corresponding author: Ibrahim Abbas, Mathematics Department, Faculty of Science, Sohag University, Sohag, Egypt, e-mail: ibrabbas7@science.sohag.edu.eg

**Zuhur Alqahtani:** Department of Mathematical Sciences, College of Science, Princess Nourah bint Abdulrahman University, P.O. Box 84428, Riyadh, 11671, Saudi Arabia, e-mail: zumalqahtani@pnu.edu.sa

Alaa A. El-Bary: Institute of Basic and Applied Science, Arab Academy for Science, Technology and Maritime Transport, Alexandria, Egypt, e-mail: aaelbary@aast.edu

**Areej Almuneef:** Department of Mathematical Sciences, College of Science, Princess Nourah bint Abdulrahman University, P.O. Box 84428, Riyadh, 11671, Saudi Arabia, e-mail: aaalmuneef@pnu.edu.sa

 $I_o$  Laser intensity

 $t_p$  Laser pulse time duration

 $a_t$  Linear thermal expansion coefficient

T Medium temperature

Specific heat

 $e_{ij}$  Strain components

 $\sigma_{ij}$  Stress components

 $R_a$  Surface reflectivity

 $K^*$  The additional material constant

The length

 $\rho$  The mass density

t The time

## 1 Introduction

Functionally graded material (FGM) is a unique composite material whose volume fractions of different composite elements continuously shift from side to side. It was first developed as a heat barrier material for aircraft projects [1]. Because of its remarkable thermo-mechanical properties, this novel inhomogeneous medium can withstand high temperatures. Pressure tanks, chemical plants, pipelines, nuclear reactors, airplanes other vital constructions are among the many important structures that employ them. One of the most intriguing aspects of FGMs is the ability to engineer their property gradient. This gradation may be produced using a variety of functional forms, with exponential variation garnering the most interest. The exponential variation of material features in FGMs improves stress distributions and minimizes stress concentration, allowing for smooth transitions between different components or phases. This is especially useful when mechanical stresses and significant temperature gradients are present. Considerable progress has been made in researching non-homogeneous FGMs with exponential fluctuations in their characteristics. Researchers have investigated a variety of analytical and numerical techniques to comprehend how these materials behave under varied loading and environmental circumstances. The material's exponential gradation is very appropriate for applications in the aerospace, automotive, and civil engineering industries because it provides special

benefits for adjusting the material's response to mechanical and thermal stresses.

In 1991, Green and Naghdi [2] introduced three significant theories for generalized thermoelastic in isotropic and homogeneous media, which they labeled as Models GNI, GNII, and GNIII. The primary distinction among these models lies in their handling of heat conduction and thermal wave propagation. Model GNI reduces to the classical heat conduction model, which is upon Fourier's law, when the corresponding theories are linearized. This model maintains the traditional view of heat transfer, where thermal disturbances propagate instantaneously, leading to infinite speeds of thermal wave propagation. In contrast, the linearized model versions GNII and GNIII permit the propagation of thermal waves at finite speeds, thus addressing a key limitation of the classical theory. Specifically, Model GNII offers a novel characteristic not seen in other well-established thermoelastic theories: it does not allow heat energy to dissipate. As explained in detail in Green and Naghdi's later studies [3,4], this model incorporates the gradient of thermal displacement among other constitutive variables and derives its constitutive equations beginning with the reduced energy formulation. The dynamic response, thermoelastic behavior, and failure mechanisms of exponentially graded FGMs have been the subject of recent studies. These studies have shown that by improving the stress distribution and lowering the chance of failure, exponential grading may greatly improve the material's performance. Furthermore, the advent of sophisticated computational approaches has made it possible to model and simulate FGMs more accurately, giving researchers a better understanding of their intricate behavior.

No transient thermoelastic problems involving functionally graded materials have, as far as the authors are aware, been resolved using generalized thermoelastic models in the absence of energy dissipation (GNII model). The thermomechanical issue of FGM hollow cylinders, whose material characteristics are supposed to be temperature-independent and to fluctuate continuously in the radial directions, was addressed by Shao et al. [5]. A finite difference approach was used by El-Naggar et al. [6] to investigate the transient thermal stress in inhomogeneous orthotropic cylinders. The one-dimensional thermal stress of functionally graded spheres [7] and cylinders [8], whose elastic modulus and linear thermal expansion coefficients change linearly with radius, have accurate solutions given by Lutz and Zimmerman. Using perturbation methods, Obata and Noda [9] have studied the 1D functionally graded hollow sphere and hollow cylinder. Qian and Batra [10] and Vel and Batra [11] examined the 3D constant or transient thermal stresses problem of functionally graded rectangular plates, whose

material properties vary with the power product form across the thicknesses. However, the thermoelastic analysis of cylindrical panels composed of FGM, spheres, and circular cylinders becomes significant due to the widespread application of shell-type structures in numerous industrial domains. Sankar and Tzeng [12] investigated the issue of thermal disturbances in functionally graded beams with two-dimensional steady state and with differences in thermoelectric properties which vary exponentially with thickness. The stable thermoelastic issues of nonhomogeneous slabs were analytically treated by Jeon et al. [13], assuming that the thermal conductivity, the coefficient of linear thermal expansion, and the shear elastic modulus change with the power product form of the axial coordinate variable. In a study conducted by Sugano [14], the transient thermal stress issue of an inhomogeneous plate in one dimension was examined. Othman and Abbas [15] studied the thermoelastic interactions with energy dissipation in an inhomogeneous isotropic hollow cylinder. Gunghas et al.'s study on the impact of magnetic field on functionally graded thermoelastic material [16]. In viscoelastic functionally graded plates, Sur and Kanoria [17] demonstrated thermoelastic interaction. Abbas [18] investigated the impacts of relaxation times in an inhomogeneous hollow cylinder by the finite element approach. Reddy and Chin [19] examined thermomechanical interaction in functionally graded cylinders and plates. Abbas and Zenkour [20] have applied the Lord and Shulman model for the magneto-electrothermoelastic responses of infinite functionally graded cylinders.

Numerous researchers have examined potential solutions to numerous problems in the context of various generalized thermoelasticity theories. The different aspects of the problem are examined in these studies by using more complicated models like hyperbolic two-temperature photothermal interaction in semiconductors media [21,22], vibrational analysis of microbeams with two temperatures [23], or thermoelectric phonon coupling in metals [24,25]. The theories of the GreenLindsay model have also changed with constraints in the continuity of Green-Lindsay structural analysis model have been introduced with force modification [26]. The models of isotropic and transversely isotropic plates in terms of nonlocality, rotation and two-temperature effects have also been examined going further from modification [27–29]. Most other authors have also investigated the microstructure and intrinsic rotation and contraction in thermoelastic bodies [30,31] and deformation of voided thermoelastic dipolar material [32]. In other studies, furthermore, finite element techniques were used to nonlinear dual-phase lag bioheat models which assisted in heat transfer formulations to living tissues [33,34] whereas, fractional order three-phase lag models were used to

study mechanical thermal stress in microstructures with non-homogenous materials [35]. Generalized thermoelasticity framework has been employed to model microscale beams with moving heat sources [36]. Nonlinear thermodynamics of laser bioheat models analyzed the biological effects of laser on biological tissues [37]. There has also been some research in thermomechanical analysis of shells made of laminated composites and FGMs. Use of the equivalent layer-wise formulation [38,39]. By the testing of 3D shell models within the framework of the thermomechanical modeling of FGM structures, predictors of the thermoelastic models have been improved in many aspects [40,41].

The present work is to investigate non-homogeneous FGMs with exponential fluctuations in more detail to better understand their features and potential uses. This work aims to clarify the impact of exponential gradation on the thermo-mechanical performance of the material by using both numerical and analytical methods, providing important information for the development and refinement of sophisticated engineering materials.

## 2 Basic equations

With timed pulse heat sources dispersed throughout a plane region, we examine functionally graded materials isotropic indefinitely extended thermoelastic medium with an uniform reference temperature  $T_o$ . The Green-Naghdi model GNII (TEWED)-based dynamic coupled generalized thermoelasticity's governing field equations are expressed as [3,4]:

$$\sigma_{ij,j} = \rho \frac{\partial^2 u_i}{\partial t^2}, \quad i = 1, 2, 3,$$
 (1)

$$(K^*T_i)_i = \rho c_e \frac{\partial^2 T}{\partial t^2} + \gamma T_o \frac{\partial^2 u_{i,i}}{\partial t^2} - \frac{\partial Q}{\partial t}, \quad i = 1, 2, 3, \quad (2)$$

$$\sigma_{ij} = \mu(u_{i,j} + u_{j,i}) + (\lambda u_{k,k} - \gamma (T - T_o))\delta_{ij}. \tag{3}$$

Since f(X) is a defined nondimensional function of the space variables X = (x, y, z), we replace  $K^*, y, \mu, \lambda$ , and  $\rho$  with  $K_o^*(X)$ ,  $\gamma_o(X)$ ,  $\mu_o(X)$ ,  $\lambda_o(X)$ , and  $\rho_o(X)$ , where  $K_o^*$ ,  $\gamma_o$ ,  $\mu_o$ ,  $\lambda_o$ , and  $\rho_o$  are regarded as constants. Then, for Eqs. (1)–(3), the following form is assumed:

$$f(X)[\mu_{o}(u_{i,j} + u_{j,i}) + (\lambda_{o}u_{k,k} - \gamma_{o}(T - T_{o}))\delta_{ij}]_{j} + f(X)_{j}[(\lambda_{o}u_{k,k} - \gamma_{o}(T - T_{o}))\delta_{ij} + \mu_{o}(u_{i,j} + u_{j,i})] = \rho_{o}f(X)\frac{\partial^{2}u_{i}}{\partial t^{2}}, \quad i = 1, 2, 3,$$
(4)

$$(K_o^* f(X) T_j)_j = \rho_o c_e f(X) \frac{\partial^2 T}{\partial t^2} + T_o \gamma_o f(X) \frac{\partial^2 u_{i,i}}{\partial t^2} - \frac{\partial Q}{\partial t},$$

$$j = 1, 2, 3,$$
(5)

$$u(0,t)=0, \frac{\partial T(0,t)}{\partial x}=0$$
 $X$ 

Functionally graded material

 $u(l,t)=0, \frac{\partial T(l,t)}{\partial x}=0$ 

Figure 1: Schematic of the problem.

$$\sigma_{ij} = f(X)[\mu_o(u_{i,j} + u_{j,i}) + (\lambda_o u_{k,k} - \gamma_o(T - T_o))\delta_{ij}].$$
 (6)

## 3 Formulations of the problem

An isotropic thermoelastic functionally graded medium is the subject of the study. The half-space's bounding plane points inward when the x-axis is taken perpendicular to it, and this is the region where it is situated,  $0 \le x \le l$ , as in Figure 1.

Temperature T and displacement vector  $\vec{u}$  may be expressed as follows, assuming that the state of the material depends solely on x and t:

$$T = T(x, t), \quad \overrightarrow{u} = (u(x, t), 0, 0).$$
 (7)

Presumably, the only variable affecting the properties of the material is the x-coordinate. As a result, we regard f(X) as f(x). The constitutive equation, the motion equation, and the heating conduction relation in the context of the generalized thermoelastic theory upon one GNII model can be stated by

$$f(x)\left[(\lambda_o + 2\mu_o)\frac{\partial^2 u}{\partial x^2} - \gamma_o \frac{\partial T}{\partial x}\right] + \left[(\lambda_o + 2\mu_o)\frac{\partial u}{\partial x} - \gamma_o (T - T_o)\right] = \rho_o f(x)\frac{\partial^2 u}{\partial t^2}$$
(8)

$$K_o^* f(x) \frac{\partial^2 T}{\partial x^2} + K_o^* \frac{\partial f(x)}{\partial x} \frac{\partial T}{\partial x}$$

$$= \rho_o c_e f(x) \frac{\partial^2 T}{\partial t^2} + \gamma_o T_o f(x) \frac{\partial^3 u}{\partial t^2 \partial x} - \frac{\partial Q}{\partial t}$$
(9)

$$\sigma_{xx} = f(x) \left[ (\lambda_o + 2\mu_o) \frac{\partial u}{\partial x} - \gamma_o (T - T_o) \right]$$
 (10)

Now, let us suppose that  $f(x) = e^{ax}$ , where a is a constant without dimensions [42] and the energy source, Q(x, t), on the surface of the material may be used to characterize conduction heat transfer as a one-dimensional problem [43]:

$$Q(x,t) = \frac{R_a I_o t}{\delta t_p^2} e^{-\frac{t}{t_p}} e^{-\frac{x}{\delta}}$$
(11)

Next, simplifying Eqs. (8)-(10) to

$$\left[ (\lambda_o + 2\mu_o) \frac{\partial^2 u}{\partial x^2} - \gamma_o \frac{\partial T}{\partial x} \right] + a \left[ (\lambda_o + 2\mu_o) \frac{\partial u}{\partial x} \right] 
- \gamma_o (T - T_o) = \rho_o \frac{\partial^2 u}{\partial t^2}$$
(12)

$$K_o^* \frac{\partial^2 T}{\partial x^2} + K_o^* a \frac{\partial T}{\partial x} = \rho_o c_e \frac{\partial^2 T}{\partial t^2} + \gamma_o T_o \frac{\partial^3 u}{\partial t^2 \partial x} - e^{-ax} \frac{\partial}{\partial t} \left[ \frac{R_a I_o t}{\delta t_p^2} e^{-\frac{t}{t_p}} e^{-\frac{x}{\delta}} \right]$$
(13)

$$\sigma_{xx} = e^{ax} \left[ (\lambda_o + 2\mu_o) \frac{\partial u}{\partial x} - \gamma_o (T - T_o) \right]$$
 (14)

# 4 Initial and boundary conditions

The formulae can only be solved if the beginning and boundary criteria listed below are met:

$$u(x,0) = 0, \quad T(x,0) = T_0, \quad \frac{\partial T(x,0)}{\partial t} = 0,$$

$$\frac{\partial u(x,t)}{\partial t} = 0$$
(15)

$$u(0,t)=0, \quad \frac{\partial T(0,t)}{\partial x}=0, \quad u(l,t)=0, \quad \frac{\partial T(l,t)}{\partial x}=0$$
 (16)

The basic equations might be made simpler by using these dimensionless variables.

$$T' = \frac{T - T_0}{T_0}, \quad t' = \frac{c}{l}t, \quad x' = \frac{x}{l},$$

$$u' = \frac{\lambda_0 + 2\mu_0}{lv T_0}, \quad \sigma'_{xx} = \frac{\sigma_{xx}}{v T_0}, \quad Q' = \frac{l}{\rho_0 c_0 T_0 c}Q,$$

$$(17)$$

where  $c^2 = \frac{\lambda_o + 2\mu_o}{\rho_o}$  and  $\gamma_o = (3\lambda_o + 2\mu_o)\alpha_t$ . Eqs. (12)–(14) with the starting (15) and boundary (16) conditions added after the primes are suppressed yield

$$\frac{\partial^2 u}{\partial x^2} - \frac{\partial T}{\partial x} + a \left[ \frac{\partial u}{\partial x} - T \right] = \frac{\partial^2 u}{\partial t^2}$$
 (18)

$$\varepsilon_{1} \frac{\partial^{2} T}{\partial x^{2}} + \varepsilon_{1} a \frac{\partial T}{\partial x} = \frac{\partial^{2} T}{\partial t^{2}} + \varepsilon_{2} \frac{\partial^{3} u}{\partial t^{2} \partial x} - \frac{R_{a} L_{o(t_{p}-t)}}{\delta t_{p}^{3}} e^{-\zeta x}$$
(19)

$$\sigma_{xx} = e^{ax} \left( \frac{\partial u}{\partial x} - T \right) \tag{20}$$

$$T(x, 0) = 0,$$
  $\frac{\partial T(x, 0)}{\partial t} = 0,$   $u(x, 0) = 0,$   $\frac{\partial u(x, t)}{\partial t}$  (21)

$$u(0, t) = 0,$$
  $\frac{\partial T(0, t)}{\partial x} = 0,$   $u(l, t) = 0,$   $\frac{\partial T(l, t)}{\partial x}$  (22)

where

$$\varepsilon_1 = \frac{K_o^*}{\rho_o c_e c^2}, \quad \varepsilon_2 = \frac{\gamma_o^2 T_o}{\rho_o c_e (\lambda_o + 2\mu_o)}, \quad \zeta = \frac{\delta a - 1}{\delta}.$$

Applying Laplace transforms to Eqs. (18)–(22) may result in the following:

$$\frac{\mathrm{d}^2 \bar{u}}{\mathrm{d}x^2} = s^2 \bar{u} + a\bar{T} - a\frac{\mathrm{d}\bar{u}}{\mathrm{d}x} + \frac{\mathrm{d}\bar{T}}{\mathrm{d}x} \tag{23}$$

$$\frac{\mathrm{d}^2 \bar{T}}{\mathrm{d}x^2} = \frac{s^2}{\varepsilon_1} \bar{T} + \frac{s^2 \varepsilon_2}{\varepsilon_1} \frac{\mathrm{d}\bar{u}}{\mathrm{d}x} - a \frac{\mathrm{d}\bar{T}}{\mathrm{d}x} - \frac{s R_a I_o}{\delta \varepsilon_1 (1 + s t_p)^2} \mathrm{e}^{-\zeta x} \quad (24)$$

$$\bar{\sigma}_{xx} = e^{ax} \left( \frac{d\bar{u}}{dx} - \bar{T} \right)$$
 (25)

$$\bar{u}(0,s) = 0$$
,  $\frac{d\bar{T}(0,s)}{dx} = 0$ ,  $\bar{u}(l,s) = 0$ ,  $\frac{d\bar{T}(l,s)}{dx} = 0$  (26)

Combining formulations (23) and (24) yields the following expression for the vector-matrix differential equations:

$$\frac{\mathrm{d}M}{\mathrm{d}x} = AM - g\mathrm{e}^{-\zeta x} \tag{27}$$

where 
$$M = \begin{bmatrix} \overline{u} \\ \overline{T} \\ \frac{d\overline{u}}{dx} \\ \frac{dT}{dx} \end{bmatrix}$$
,  $A = \begin{bmatrix} 0 & 0 & 1 & 0 \\ 0 & 0 & 0 & 1 \\ s^2 & a & -a & 1 \\ 0 & b_1 & b_2 & -a \end{bmatrix}$ ,  $g = \begin{bmatrix} 0 \\ 0 \\ b_3 \end{bmatrix}$ ,  $b_1 = \frac{s^2}{\varepsilon_1}$ ,

$$b_2 = \frac{s^2 \varepsilon_2}{\varepsilon_1}, b_3 = \frac{s R_a I_o}{\delta \varepsilon_1 (1 + s t_n)^2}.$$

The eigenvalues approach has been successfully used to represent the characteristic equation of matrix A in terms of the solution obtained from (27) as previously stated in works [35,44]. As a result, the following is the distinctive formulation of the A matrix:

$$\omega^4 + 2a\omega^3 + \omega^2(a^2 - s^2 - b_1 - b_2) - (as^2 + ab_1 + ab_2)\omega + s^2b_1 = 0$$
(28)

The eigenvalues of matrix A are determined by the four roots of the equation, denoted as  $\omega_1$ ,  $\omega_2$ ,  $\omega_3$ ,  $\omega_4$ . The solutions to this equation are as follows:

The eigenvalues of matrix A are determined by the four roots of the equation, denoted by the symbols  $\omega_1$ ,  $\omega_2$ ,  $\omega_3$ , and  $\omega_4$ . The solutions of this problem may be given by:

$$M(x,s) = \sum_{i=1}^{4} B_i Y_i e^{\omega_i x} + f e^{-\zeta x}$$
 (29)

The problem boundary conditions represent the constants  $B_1, B_2, B_3, B_4$  and  $f = [f_1, f_2, f_3, f_4]^T$ , where  $f_1 = [f_1, f_2, f_3, f_4]^T$  $f_3 = -\zeta f_1$  $\overline{((a-\zeta)\zeta+s^2)((a-\zeta)\zeta+b_1)+(a-\zeta)\zeta b_2},$  $b_3((a-\zeta)\zeta+s^2)$  $\frac{\sum_{3 \le (\alpha - \zeta)\zeta + s^2)((\alpha - \zeta)\zeta + s^2)}{((\alpha - \zeta)\zeta + s^2)((\alpha - \zeta)\zeta + b_1) + (\alpha - \zeta)\zeta b_2}, f_4 = -\zeta f_2.$ 

**DE GRUYTER** 

Numerical inversion methods were used to find the general solution's displacement, temperature, and stress distribution. The use of Riemann-sum approximation methods allowed for the observation of the numerical findings. The following method was used to translate the function from the Laplace domain to the time domains:

$$V(x,t) = \frac{e^{pt}}{t} \left( \frac{1}{2} \operatorname{Re}\left[\overline{V}(x,p)\right] + \operatorname{Re}\sum_{n=0}^{N} (-1)^n \overline{V}\left[x, p + \frac{in\pi}{t}\right] \right)$$
(30)

Here, the real component is represented by Re, while the imaginary unit is denoted by i. Equation [45] is satisfied when p = 4.7/t is used, as shown by numerical testing.

## 5 Numerical results

This work applies extended thermoelastic theory without energy dissipation to an isotropic medium and examines the thermoelastic responses to laser heat sources with timed pulse. An outline of the material specifications is provided below [18]:

$$\lambda_o = 7.76 \times 10^{10} \text{ kg m}^{-1} \text{ s}^{-2}$$
  
 $\mu_o = 3.86 \times 10^{10} \text{ kg m}^{-1} \text{ s}^{-2}$   
 $t_p = 0.2, t = 0.3$ 

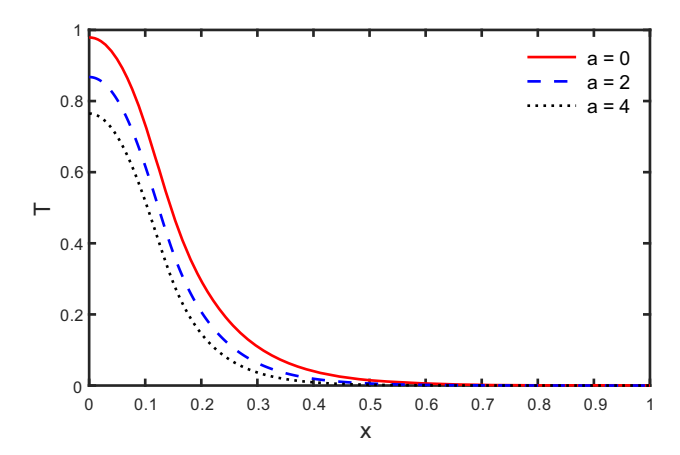


Figure 2: The impacts of non-homogeneity on temperature variation.

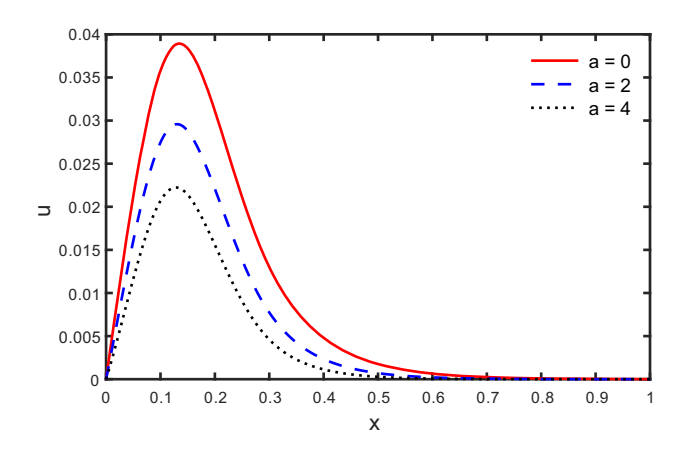


Figure 3: The impacts of non-homogeneity on the variation of displacement.

$$\rho_o = 8.954 \times 10^3 \text{ kg m}^{-3}$$
 $T_0 = 293 \text{ K}, \quad \delta = 0.1$ 
 $K_o = 3.86 \times 10^2 \text{ kg m K}^{-1} \text{ s}^{-3}$ 
 $c_e = 3.8310 \times 10^2 \text{ m}^2 \text{ K}^{-1} \text{ s}^{-2}$ 
 $\alpha_t = 17.8 \times 10^{-6} \text{ K}^{-1}, \quad R_a = 0.5$ 

The generalized thermoelastic model without energy dissipation is used to numerically calculate the physical parameters for the distance x as in Figures 2–10. The purpose of this study is to examine how nonhomogeneity affects temperature, stress, and thermal displacement for FGMs. The findings are shown graphically in Figures 2-4. The temperature, thermal displacement, and stress under (GN II model) variation for time t = 0.3 and nonhomogeneity parameter a = 0, 2, and 4 is shown in Figures 2–4. To investigate how nonhomogeneity affects temperature T with distance x, Figure 2 is shown. As x increases, the temperatures first approach maximum values, satisfying the given boundary requirements, and then, they progressively decrease until

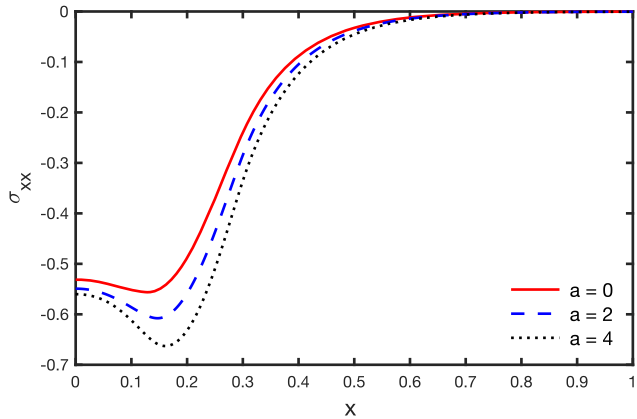
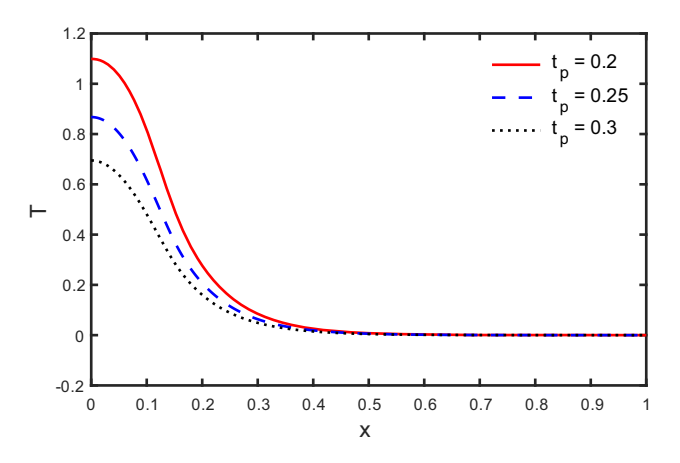
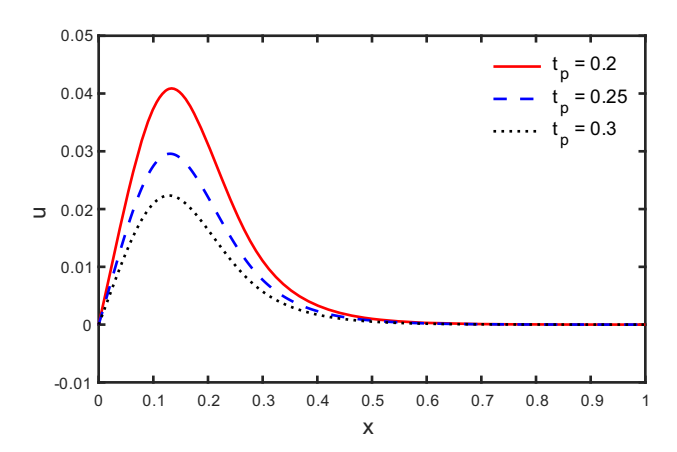


Figure 4: The impacts of non-homogeneity on the stress variation.



**Figure 5:** The impacts of laser pulse time duration on temperature variation.



**Figure 6:** The impacts of laser pulse time duration on displacement variations.

they approach zeros. It is found that for a certain x, the magnitude of T decreases with the nonhomogeneity parameter and that at this value, the magnitude of T goes to zero. The

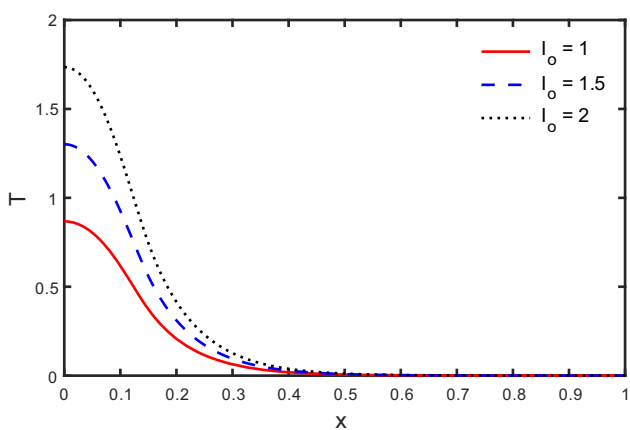
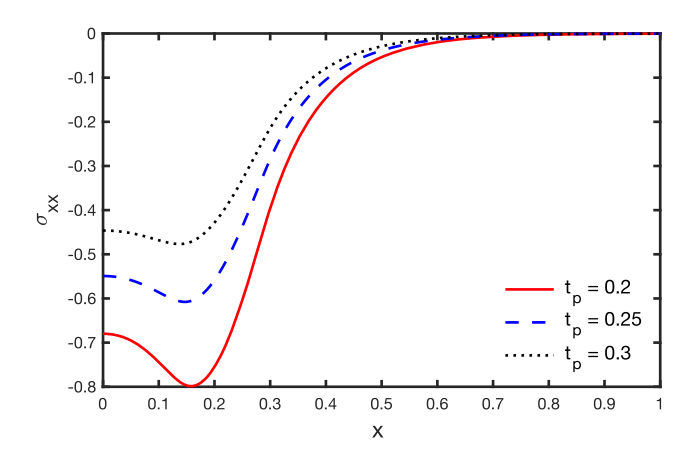


Figure 8: The impacts of laser intensity on temperature variations.

change of thermal displacement u vs x is shown in Figure 3, where the nonhomogeneity parameter is assumed to be a = 0, 2, and 4 for (GN II model) to investigate the impact of nonhomogeneity in the range  $0 \le x \le 1$ . As can be seen from the figure, the displacement starts from zeros according to the problem boundary conditions and then the displacement will rise to a maximum close to x = 0.15 and then decline to zero. It is also noted that in this model, the displacement component's peak magnitude would decrease with an increase in the nonhomogeneity parameter.

The thermal stress variation  $\sigma_{xx}$  vs distance x is shown in Figure 4. It is evident that the stress follows a pattern, starting its peak at negative values before steadily declining to practically zero. Figures 5–7 illustrate how the length of the laser pulse under inhomogeneity affects the stress distribution, temperature, and displacement. As expected, there are significant impacts of the laser pulse duration on the temperature, displacement, and stress distributions. Based on the results, Figures 8–10 illustrate how all physical quantities fluctuate along the distances x for various laser



**Figure 7:** The impacts of laser pulse time duration on the stress variation.

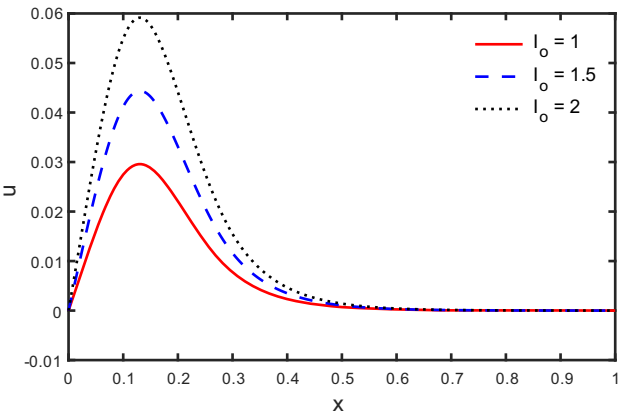


Figure 9: The impacts of laser intensity on the displacement variation.

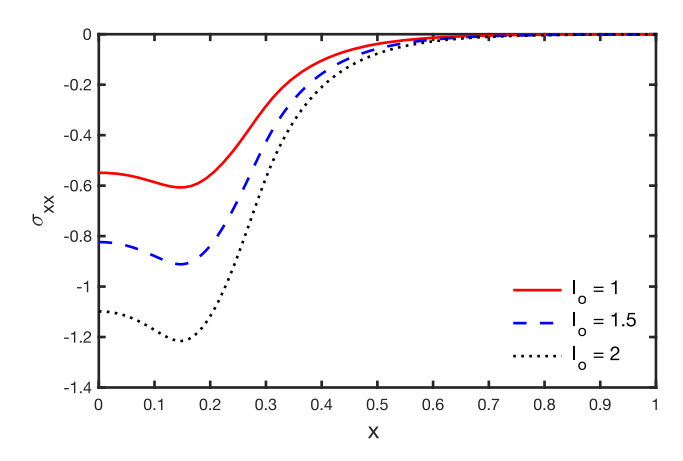


Figure 10: The impacts of laser intensity on the stress variation.

intensity values under non-homogeneity. Based on these results, it can be said that all of the physical quantities are significantly impacted by the laser's intensity when it is exposed to non-homogeneity.

### 6 Conclusion

The investigation establishes that the factors of nonhomogeneity, the duration of laser pulses, and the level of laser beam focus play a significant role during the thermoelastic responses of the FGMs. The approach of GNII model has been useful in explaining how these effects combine and influence the temperature, stress and displacement distribution. The results lead to the following conclusions:

- Nonhomogeneity significantly influences the temperature, thermal displacement, and stress distributions. As the nonhomogeneity parameter increases, both temperature and thermal displacement decrease, resulting in reduced material deformation and stress.
- Temperature peaks at the surface and then declines to zero as xx increases. This behavior becomes more pronounced with higher nonhomogeneity.
- Displacement reaches a maximum at a particular distance before decreasing, with larger nonhomogeneity causing a reduction in the peak displacement.
- Stress follows a similar pattern, starting with a negative peak and decreasing towards zero, with higher nonhomogeneity resulting in smaller stress magnitudes.
- The length of the laser pulse greatly impacts the thermoelastic responses. Longer laser pulses lead to higher values of temperature, displacement, and stress in nonhomogeneous materials.
- Increasing laser intensity leads to stronger variations in displacement, temperature, and stress distributions, particularly

in the presence of nonhomogeneity, highlighting the significant effect of laser power on the thermoelasticity behavior of FGMs.

**Acknowledgements:** Princess Nourah bint Abdulrahman University Researchers Supporting Project number (PNURSP2024R518), Princess Nourah bint Abdulrahman University, Riyadh, Saudi Arabia.

**Funding information:** Princess Nourah bint Abdulrahman University Researchers Supporting Project number (PNURSP2024R518), Princess Nourah bint Abdulrahman University, Riyadh, Saudi Arabia.

**Author contributions:** All authors have accepted responsibility for the entire content of this manuscript and consented to its submission to the journal, reviewed all the results, and approved the final version of the manuscript. Conceptualization: ZA, IA, and AA; methodology: ZA, IA, and AAE-B; software: ZA, IA, and AAE-B; validation: IA, AAE-B, and AA; formal analysis: IA, AAE-B, and AA; investigation: ZA, IA, AAE-B, and AA; resources: AA.

Conflict of interest: Authors state no conflict of interest.

#### References

- [1] Delfosse D. Fundamentals of Functionally Graded Materials | S.
   Suresh and A. Mortensen IOM Communications Ltd, 1998 ISBN:
   1-86125-063-0. Elsevier; 1998.
- [2] Green AE, Naghdi P. A re-examination of the basic postulates of thermomechanics. Proc R Soc Lond Ser A: Math Phys Sci. 1991;432(1885):171–94.
- [3] Green AE, Naghdi PM. On undamped heat waves in an elastic solid.J Therm Stresses. 1992;15(2):253–64.
- [4] Green AE, Naghdi PM. Thermoelasticity without energy dissipation.| Elast. 1993;31(3):189–208.
- [5] Shao Z, Wang T, Ang K. Transient thermo-mechanical analysis of functionally graded hollow circular cylinders. J Therm Stresses. 2007;30(1):81–104.
- [6] El-Naggar A, Abd-Alla A, Fahmy M, Ahmed S. Thermal stresses in a rotating non-homogeneous orthotropic hollow cylinder. Heat Mass Transf. 2002;39(1):41–6.
- [7] Lutz MP, Zimmerman RW. Thermal stresses and effective thermal expansion coefficient of a functionally gradient sphere. J Therm Stresses. 1996;19(1):39–54.
- [8] Zimmerman RW, Lutz MP. Thermal stresses and thermal expansion in a uniformly heated functionally graded cylinder. J Therm Stresses. 1999;22(2):177–88.
- [9] Obata Y, Noda N. Steady thermal stresses in a hollow circular cylinder and a hollow sphere of a functionally gradient material. J Therm Stresses. 1994;17(3):471–87.
- [10] Qian LF, Batra RC. Transient thermoelastic deformations of a thick functionally graded plate. J Therm Stresses. 2004;27(8):705–40.

- [11] Vel SS, Batra R. Exact solution for thermoelastic deformations of functionally graded thick rectangular plates. AIAA J. 2002;40(7):1421–33.
- [12] Sankar BV, Tzeng JT. Thermal stresses in functionally graded beams. AIAA J. 2002;40(6):1228–32.
- [13] Jeon SP, Tanigawa Y, Sone D. Analytical treatment of axisymmetrical thermoelastic field with kassir's nonhomogeneous material properties and its adaptation to boundary value problem of slab under steady temperature field. J Therm Stresses. 1997;20(3–4):325–43.
- [14] Sugano Y. An expression for transient thermal stress in a nonhomogeneous plate with temperature variation through thickness. Ing-Archiv. 1987;57(2):147–56.
- [15] Othman MIA, Abbas IA. Generalized thermoelasticity of thermalshock problem in a non-homogeneous isotropic hollow cylinder with energy dissipation. Int J Thermophys. 2012;33(5):913–23.
- [16] Gunghas A, Kumar R, Deswal S, Kalkal KK. Influence of rotation and magnetic fields on a functionally graded thermoelastic solid subjected to a mechanical load. J Math. 2019;2019(1):1016981.
- [17] Sur A, Kanoria M. Thermoelastic interaction in a viscoelastic functionally graded half-space under three-phase-lag model. Eur J Comput Mech. 2014;23(5–6):179–98.
- [18] Abbas IA. Generalized magneto-thermoelasticity in a nonhomogeneous isotropic hollow cylinder using the finite element method. Arch Appl Mech. 2009;79(1):41–50.
- [19] Reddy JN, Chin CD. Thermomechanical analysis of functionally graded cylinders and plates. J Therm Stresses. 1998;21(6):593–626.
- [20] Abbas IA, Zenkour AM. LS model on electro-magneto-thermoelastic response of an infinite functionally graded cylinder. Compos Struct. 2013;96:89–96.
- [21] Abbas I, Saeed T, Alhothuali M. Hyperbolic two-temperature photothermal interaction in a semiconductor medium with a cylindrical cavity. Silicon. 2020;13(6):1871–8.
- [22] Alzahrani FS, Abbas IA. Photo-thermal interactions in a semiconducting media with a spherical cavity under hyperbolic two-temperature model. Mathematics. 2020;8(4):585.
- [23] Carrera E, Abouelregal AE, Abbas IA, Zenkour AM. Vibrational analysis for an axially moving microbeam with two temperatures. J Therm Stresses. 2015;38(6):569–90.
- [24] Wu H, Li X, Yu Y, Deng Z. A novel electron-phonon coupling thermoelasticity with Burgers electronic heat transfer. Appl Math Mech. 2023;44(11):1927–40.
- [25] Yu YJ, Deng ZC. New insights on microscale transient thermoelastic responses for metals with electron-lattice coupling mechanism. Eur J Mech – A/Solids. 2020;80:103887.
- [26] Yu YJ, Xue Z-N, Tian X-G. A modified Green–Lindsay thermoelasticity with strain rate to eliminate the discontinuity. Meccanica. 2018;53(10):2543–54.
- [27] Lata P, Kaur H. Interactions in a transversely isotropic new modified couple stress thermoelastic thick circular plate with two temperature theory. Coupled Syst Mech. 2023;12(3):261–76.

- [28] Lata P, Singh S. Effect of rotation and inclined load in a nonlocal magnetothermoelastic solid with two temperature. Adv Mater Res. 2022;11(1):23.
- [29] Singh S, Lata P. Effect of two temperature and nonlocality in an isotropic thermoelastic thick circular plate without energy dissipation. Partial Differ Equ Appl Math. 2023;7:100512.
- [30] Marin M, Abbas I, Kumar R. Relaxed Saint-Venant principle for thermoelastic micropolar diffusion. Struct Eng Mech. 2014;51(4):651–62.
- [31] Marin MI, Agarwal RP, Abbas IA. Effect of intrinsic rotations, microstructural expansion and contractions in initial boundary value problem of thermoelastic bodies. Bound Value Probl. 2014;2014:1–16.
- [32] Marin M, Abbas I, Vlase S, Craciun EM. A study of deformations in a thermoelastic dipolar body with voids. Symmetry. 2020;12(2):267.
- [33] Marin M, Hobiny A, Abbas I. Finite element analysis of nonlinear bioheat model in skin tissue due to external thermal sources. Mathematics. 2021;9(13):1459.
- [34] Saeed T, Abbas I. Finite element analyses of nonlinear DPL bioheat model in spherical tissues using experimental data. Mech Based Des Struct Mach. 2022;50(4):1287–97.
- [35] Abbas IA. Generalized thermoelastic interaction in functional graded material with fractional order three-phase lag heat transfer. J Cent South Univ. 2015;22(5):1606–13.
- [36] Abbas IAA. GN model for thermoelastic interaction in a microscale beam subjected to a moving heat source. Acta Mech. 2015;226(8):2527–36.
- [37] Hobiny AD, Abbas IA. Nonlinear analysis of dual-phase lag bio-heat model in living tissues induced by laser irradiation. J Therm Stresses. 2020;43(4):503–11.
- [38] Tornabene F, Viscoti M, Dimitri R. Thermo-mechanical analysis of laminated doubly-curved shells: Higher order equivalent layer-wise formulation. Compos Struct. 2024;335:117995.
- [39] Mangala A, Jayasuriya M, Dwivedi SN, Louisiana L, Sivaneri NT, Lyons DW. Doubly curved laminated composite shells with hygrothermal conditioning and dynamic loads, part 2: FEA and numerical results of shells of revolution. Mech Adv Mater Struct. 2002;9(1):69–97.
- [40] Brischetto S, Torre R. 3D shell model for the thermo-mechanical analysis of FGM structures via imposed and calculated temperature profiles. Aerosp Sci Technol. 2019;85:125–49.
- [41] Tornabene F, Viscoti M, Dimitri R. Equivalent layer-wise theory for the hygro-thermo-magneto-electro-elastic analysis of laminated curved shells. Thin-Walled Struct. 2024;198:111751.
- [42] Mallik SH, Kanoria M. Generalized thermoelastic functionally graded solid with a periodically varying heat source. Int J Solids Struct. 2007;44(22):7633–45.
- [43] Sun Y, Fang D, Saka M, Soh AK. Laser-induced vibrations of microbeams under different boundary conditions. Int J Solids Struct. 2008;45(7):1993–2013.
- [44] Hobiny A, Abbas I, Marin M. The influences of the hyperbolic twotemperatures theory on waves propagation in a semiconductor material containing spherical cavity. Mathematics. 2022;10(1):121.
- [45] Tzou DY. Macro-to micro-scale heat transfer: the lagging behavior. John Wiley & Son; 2014.